

Matrix Boussinesq solitons and their tropical limit

ARISTOPHANES DIMAKIS¹, FOLKERT MÜLLER-HOISSEN^{2,3}, XIAO-MIN CHEN^{2,4}

¹ Dept. of Financial and Management Engineering, University of the Aegean, Chios, Greece

² Max Planck Institute for Dynamics and Self-Organization, Göttingen, Germany

³ Institute for Nonlinear Dynamics, Georg August University, 37077 Göttingen, Germany

⁴ College of Applied Sciences, Beijing University of Technology, Beijing 100124, People's Republic of China

Abstract

We study soliton solutions of matrix “good” Boussinesq equations, generated via a binary Darboux transformation. Essential features of these solutions are revealed via their “tropical limit”, as also exploited in previous work about the KP equation. This limit associates a point particle interaction picture with a soliton (wave) solution.

1 Introduction

The (scalar) Boussinesq equation originated from the study of water waves propagating in a canal [1]. In this work we study the “good” Boussinesq equation, in which the highest derivative term has the opposite sign, as compared to the original Boussinesq equation. It also appears as a continuum limit of certain nonlinear atomic chains, see [2], for example. From a mathematical point of view, it belongs to the main examples of completely integrable PDEs. It is the second Gelfand-Dickey reduction [3] of the KP-II equation, the famous Korteweg-deVries (KdV) equation being the first. Compared with the latter, the behavior of its soliton solutions is considerably more diverse, in particular they can move in both directions, experience head-on collision, and solitons can split or merge (cf. [4, 5], also see the references cited in these papers). The scalar good Boussinesq equation is also known as “nonlinear string equation”, see e.g. [6, 7].

In the KdV and Boussinesq case, a contour plot of a soliton solution displays a localization along a piecewise linear graph in two-dimensional space-time. The definition of the “tropical limit” makes this precise and yields a method to compute it. Restricting the dependent variable to this graph, completes the tropical limit of the soliton solution, which displays the essentials of soliton interactions in a clear way. It is a very convenient tool to describe and to classify soliton solutions. The tropical limit associates with a soliton solution a point particle picture, also in the interaction region of solitons, revealing “virtual solitons” (borrowing a familiar notion from perturbative quantum field theory).

In this work we address more generally the following $m \times n$ matrix potential Boussinesq equation,

$$\phi_{tt} - 4\beta\phi_{xx} + \frac{1}{3}\phi_{xxxx} + 2(\phi_x K \phi_x)_x - 2(\phi_x K \phi_t - \phi_t K \phi_x) = 0, \quad (1.1)$$

where K is a constant $n \times m$ matrix, $\beta > 0$ (chosen as $\beta = 1/4$ in all plots in this work), and a subscript indicates a partial derivative of ϕ with respect to the respective variable x or t . We will refer to this equation as potential $\text{Bs}q_K$. It is the second Gelfand-Dickey reduction of the following KP-II equation, in a moving frame ($x \mapsto x - 3\beta t_3$, $t_2 = t$),

$$-\frac{4}{3}(\phi_{t_3} + 3\beta\phi_x)_x + \phi_{tt} + \frac{1}{3}\phi_{xxxx} + 2(\phi_x K \phi_x)_x - 2(\phi_x K \phi_t - \phi_t K \phi_x) = 0.$$

In terms of $u = 2\phi_x$, we obtain the $m \times n$ matrix Boussinesq equation, or rather Bsq_K ,¹

$$u_{tt} - 4\beta u_{xx} + \frac{1}{3}u_{xxxx} + (uKu)_{xx} - (uK(\partial^{-1}u)_t - (\partial^{-1}u)_t Ku)_x = 0.$$

For a solution u of the vector Boussinesq equation, where $n = 1$ or $m = 1$, Ku , respectively uK , is a solution of the scalar Boussinesq equation. If $m, n > 1$, we define the tropical limit graph via that of the scalar $\text{tr}(Ku)$, which is not in general a solution of the scalar Boussinesq equation. Our explorations and results fully substantiate this approach.

Our analysis largely parallels that in [8], where we explored line soliton solutions of the matrix KP-II equation in the tropical limit. There we concentrated on a class of solutions which we called “pure solitons”. Another class has been treated in [9]. Whereas pure solitons exhaust the solitons of the KdV reduction, this is not so for the Boussinesq reduction.

Matrix versions of scalar integrable equations are natural extensions and of interest as models of coupled systems. A further motivation to explore them originated from the fact that in 2-soliton scattering, in particular in case of the matrix KdV [10, 11] and the vector Nonlinear Schrödinger (NLS) equation [12, 13], in- and outgoing polarizations (values of the dependent variable attached to in- and outgoing solitons) are related by a Yang-Baxter map, a solution of the “functional” or “set-theoretic” version of the famous Yang-Baxter equation. For a matrix KP equation, a Yang-Baxter map is *not* sufficient to fully describe the situation [9]. It seems that we also have to go beyond Yang-Baxter in case of the second member in the family of Gel’fand-Dickey reductions of KP, which is the matrix Boussinesq equation.

The (quantum) Yang-Baxter equation is well-known to express integrability in two-dimensional quantum field theory and exactly solvable models of statistical mechanics. In the present work, as also e.g. in [8, 10, 11, 12, 13], we meet it in a classical context. Formally, however, soliton waves may be regarded as a sort of quantization of the point particles constituting the tropical limit.

In Section 2 we present a binary Darboux transformation for the potential Bsq_K equation (1.1). Appendix A explains its origin from a general result in bidifferential calculus [14, 15]. In this work we concentrate on the case of vanishing seed solution. This leads to two cases, treated in Sections 3 and 4. The soliton solutions, obtained via the binary Darboux transformation, depend on parameters that have to be roots of a cubic equation. We introduce a convenient parametrization of these roots (see Section 3.1) that greatly facilitates the further analysis. Section 5 contains some concluding remarks.

2 A binary Darboux transformation for the matrix Boussinesq equation

The following binary Darboux transformation is a special case of a general result in bidifferential calculus, see Appendix A. Let $N \in \mathbb{N}$. The integrability condition of the linear system

$$\begin{aligned} \theta_t &= \theta_{xx} + 2\phi_{0,x}K\theta, \\ \theta_{xxx} &= 3\beta\theta_x + \theta C - 3\phi_{0,x}K\theta_x - \frac{3}{2}(\phi_{0,t} + \phi_{0,xx})K\theta, \end{aligned} \tag{2.1}$$

where θ is an $m \times N$ and C a constant $N \times N$ matrix, is the potential Bsq_K equation for ϕ_0 . The same holds for the adjoint linear system

$$\chi_t = -\chi_{xx} - 2\chi K\phi_{0,x},$$

¹For the scalar Boussinesq equation, $x \mapsto -x$ and $t \mapsto -t$ are symmetries. In the matrix case, the first is still a symmetry, but $t \mapsto -t$ has to be accompanied by $u \mapsto u^T$.

$$\chi_{xxx} = 3\beta\chi_x + C'\chi - 3\chi_x K\phi_{0,x} + \frac{3}{2}\chi K(\phi_{0,t} - \phi_{0,xx}), \quad (2.2)$$

where χ is an $N \times n$ and C' a constant $N \times N$ matrix, in general different from C . The Darboux potential Ω satisfies the consistent $N \times N$ system of equations

$$\begin{aligned} \Omega_x &= -\chi K\theta, \\ \Omega_t &= -\chi K\theta_x + \chi_x K\theta, \\ C'\Omega + \Omega C &= -\chi K\theta_{xx} + \chi_x K\theta_x - \chi_{xx} K\theta + 3\beta\chi K\theta - 3\chi K\phi_{0,x} K\theta. \end{aligned} \quad (2.3)$$

At space-time points where Ω is invertible,

$$\phi = \phi_0 - \theta\Omega^{-1}\chi \quad (2.4)$$

is then a new solution of the potential Bsq_K equation.

Remark 2.1. Taking the transpose of the above equations, and applying the substitution $t \mapsto -t$, we see that, besides $K \mapsto K^T$, we also obtain $C' \leftrightarrow C^T$ and $\theta \leftrightarrow \chi^T$. We also note that $x \mapsto -x$, $\phi_0 \mapsto -\phi_0$, $C \mapsto -C$, $C' \mapsto -C'$ is a symmetry of the linear systems.

Remark 2.2. The equations (2.1) - (2.4) are invariant under a transformation

$$\theta \mapsto \theta A, \quad \chi \mapsto B\chi, \quad C \mapsto A^{-1}CA, \quad C' \mapsto BC'B^{-1}, \quad \Omega \mapsto B\Omega A,$$

with any invertible constant $N \times N$ matrices A and B .

Using (2.4) and the first of (2.3), we find

$$\begin{aligned} \text{tr}(K\phi) &= \text{tr}(K\phi_0) - \text{tr}(K\theta\Omega^{-1}\chi) = \text{tr}(K\phi_0) - \text{tr}(\chi K\theta\Omega^{-1}) = \text{tr}(K\phi_0) + \text{tr}(\Omega_x\Omega^{-1}) \\ &= \text{tr}(K\phi_0) + (\log \det \Omega)_x. \end{aligned}$$

Hence

$$\text{tr}(Ku) - \text{tr}(Ku_0) = 2(\log \det \Omega)_{xx}. \quad (2.5)$$

Such a formula is familiar in the scalar case, where $\det \Omega$ is the Hirota τ -function. But we will see that, also in the matrix case, $\det \Omega$ plays a crucial role. In the following we will still call it τ , after multiplication by a convenient factor, which preserves the relation (2.5).

2.1 Solutions for vanishing seed

The linear system with $\phi_0 = 0$ reads

$$\theta_t = \theta_{xx}, \quad \theta_{xxx} = 3\beta\theta_x + \theta C.$$

It possesses solutions of the form

$$\theta = \sum_a \theta_a e^{\vartheta(P_a)}, \quad (2.6)$$

where

$$\vartheta(P) = Px + P^2t, \quad (2.7)$$

and each P_a is a solution of the cubic equation

$$P_a^3 = 3\beta P_a + C. \quad (2.8)$$

The index a runs over any number of distinct roots.

Correspondingly, the adjoint linear system takes the form

$$\chi_t = -\chi_{xx}, \quad \chi_{xxx} = 3\beta\chi_x + C'\chi,$$

which is solved by

$$\chi = \sum_b e^{-\vartheta(Q_b)} \chi_b \quad (2.9)$$

if Q_b solves the cubic equation

$$Q_b^3 = 3\beta Q_b - C'. \quad (2.10)$$

The equations for the Darboux potential Ω are reduced to

$$\Omega_x = -\chi K\theta, \quad \Omega_t = -\chi K\theta_x + \chi_x K\theta, \quad C'\Omega + \Omega C = -\chi K\theta_{xx} + \chi_x K\theta_x - \chi_{xx} K\theta + 3\beta\chi K\theta.$$

Writing

$$\Omega = \Omega_0 + \sum_{a,b} e^{-\vartheta(Q_b)} W_{ba} e^{\vartheta(P_a)}, \quad (2.11)$$

these equations are solved if W_{ba} satisfies the Sylvester equation

$$Q_b W_{ba} - W_{ba} P_a = \chi_b K\theta_a, \quad (2.12)$$

and if the constant matrix Ω_0 is subject to

$$\Omega_0 C' + C\Omega_0 = 0. \quad (2.13)$$

As a consequence of the last condition, there are two major cases. In Section 3 we will address the case where $C' = -C$. Section 4 then deals with the complement.

We note that (2.5) reduces to

$$\text{tr}(Ku) = 2(\log \det \Omega)_{xx}. \quad (2.14)$$

3 The case $C' = -C$

If Ω_0 is invertible, Remark 2.2 shows that without restriction of generality we can choose $\Omega_0 = I_N$, the $N \times N$ identity matrix. (2.13) then implies $C' = -C$. The remaining freedom of transformations, according to Remark 2.2, is then given by transformations with $B = A^{-1}$. The similarity transformation $C \mapsto A^{-1}CA$ now allows us to assume that C has Jordan normal form.

P_a and Q_b are now solutions of the same cubic equation, so we can set

$$Q_a = P_a,$$

and the Sylvester equation takes the form

$$P_a W_{ab} - W_{ab} P_b = \chi_a K\theta_b.$$

If $a \neq b$ and P_a and P_b have disjoint spectrum, it is well-known that there is a solution and it is unique. In this case, the sum in the expression for θ or χ is over a disjoint set of solutions of the cubic equation.

We will restrict our considerations to *diagonal* matrices²

$$P_a = \text{diag}(p_{1,a}, \dots, p_{N,a}), \quad C = \text{diag}(c_1, \dots, c_N).$$

(2.8) then requires

$$p_{ia}^3 = 3\beta p_{ia} + c_i \quad i = 1, \dots, N. \quad (3.1)$$

We will only consider *real* roots. Writing

$$\chi_a = \begin{pmatrix} \eta_{1,a} \\ \vdots \\ \eta_{N,a} \end{pmatrix}, \quad \theta_a = (\xi_{1,a} \ \cdots \ \xi_{N,a}), \quad (3.2)$$

and $W_{ab} = (W_{ab,ij})$, we find

$$W_{ab,ij} = \frac{\eta_{ia} K \xi_{jb}}{p_{ia} - p_{jb}} \quad a \neq b, \quad p_{ia} \neq p_{jb}, \quad i, j = 1, \dots, N,$$

and thus

$$\Omega_{ij} = \delta_{ij} + \sum_{\substack{a,b \\ a \neq b}} \frac{\eta_{ib} K \xi_{ja}}{p_{ib} - p_{ja}} e^{\vartheta(p_{ja}) - \vartheta(p_{ib})} \quad i, j = 1, \dots, N.$$

3.1 A parametrization of the roots of the cubic equation

We are only interested in *real* soliton solutions, hence we restrict our analysis to *real* roots of the cubic equation and demand that there are at least two different ones. This requires $|c_i| \leq 2\beta^{3/2}$. We can then express the constants c_i as follows,

$$c_i = 2\beta^{3/2} \frac{1 - 45\lambda_i^2 + 135\lambda_i^4 - 27\lambda_i^6}{(1 + 3\lambda_i^2)^3}, \quad (3.3)$$

where λ_i are real parameters. The roots of the cubic equation (3.1) are then given by

$$p_{i,1} = -\frac{\sqrt{\beta}(1 + 6\lambda_i - 3\lambda_i^2)}{1 + 3\lambda_i^2}, \quad p_{i,2} = -\frac{\sqrt{\beta}(1 - 6\lambda_i - 3\lambda_i^2)}{1 + 3\lambda_i^2}, \quad p_{i,3} = \frac{2\sqrt{\beta}(1 - 3\lambda_i^2)}{1 + 3\lambda_i^2}. \quad (3.4)$$

All the roots satisfy $p^2 \leq 4\beta$. We have $\lim_{|\lambda_i| \rightarrow \infty} p_{ia} = \sqrt{\beta}$ for $a = 1, 2$, and $\lim_{|\lambda_i| \rightarrow \infty} p_{i,3} = -2\sqrt{\beta}$. Also see Fig. 1. The two involutive transformations

$$\lambda \mapsto -\lambda, \quad \lambda \mapsto \frac{1 - \lambda}{1 + 3\lambda} \quad (3.5)$$

generate the permutation group of the three roots.

²A treatment of the case where C contains larger than size 1 Jordan blocks is left aside in this work.

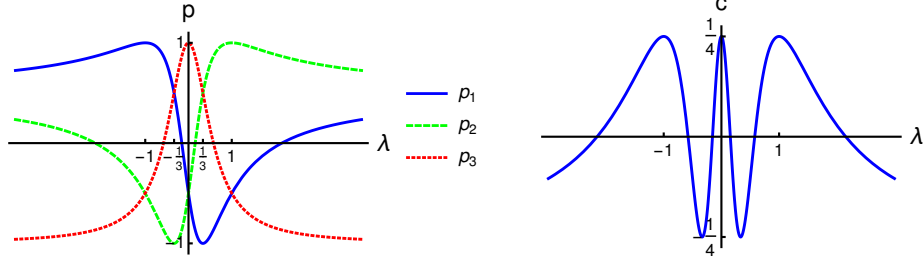


Figure 1: The roots p_a (the index i in (3.4) is suppressed), $a = 1, 2, 3$, of the cubic equation as functions of λ . The right plot shows c as a function of λ , according to (3.3). We chose $\beta = 1/4$, as also in the following figures.

3.2 Pure solitons

In this subsection we select a subclass of soliton solutions, which we call “pure solitons”. The main characterization is to restrict the expressions for the solutions of the linear systems in (2.6) and (2.9) to only involve a single root of each of the cubic equations (2.8) and (2.10). The latter equations coincide, since we assume $C' = -C$ in this section, so we have to choose two different roots, $P_1 = P$ and $P_2 = Q$, of the same cubic equation. We will further assume that these matrices are diagonal, hence

$$P = \text{diag}(p_1, \dots, p_N) =: \text{diag}(p_{1,1}, \dots, p_{N,1}),$$

$$Q = \text{diag}(q_1, \dots, q_N) =: \text{diag}(p_{1,2}, \dots, p_{N,2}).$$

It will be convenient to allow both notations for the (diagonal) entries. The constants p_i, q_i have to solve the cubic equation $z^3 = 3\beta z + c_i$. We will require $q_i \neq p_i$, $i = 1, \dots, N$. Moreover, we will mostly also assume $p_i \neq p_j$ and $q_i \neq q_j$ for $i \neq j$. Writing

$$\chi_1 = \begin{pmatrix} \eta_1 \\ \vdots \\ \eta_N \end{pmatrix}, \quad \theta_1 = (\xi_1 \quad \dots \quad \xi_N) (Q - P),$$

we then have

$$\Omega_{ij} = \delta_{ij} + w_{ij} e^{\vartheta(p_j) - \vartheta(q_i)}, \quad w_{ij} = \frac{q_j - p_j}{q_i - p_j} \eta_i K \xi_j.$$

This is exactly the expression for Ω that we found in [8] for the KP_K equation. The only difference is that, for $i = 1, \dots, N$, $q_i \neq p_i$ now have to satisfy the cubic equations, so that $p_i^3 - 3\beta p_i = q_i^3 - 3\beta q_i$ holds, which is

$$p_i^2 + p_i q_i + q_i^2 = 3\beta.$$

But, apart from this, formulae derived in [8] for the potential KP_K equation also apply to the case under consideration. Next we summarize those that are needed in this work. Introducing

$$\tau = e^{\vartheta(q_1) + \dots + \vartheta(q_N)} \det \Omega, \quad F = -e^{\vartheta(q_1) + \dots + \vartheta(q_N)} \theta e^{\vartheta(P)} \text{adj}(\Omega) e^{-\vartheta(Q)} \chi, \quad (3.6)$$

where $\text{adj}(\Omega)$ is the adjugate of the matrix Ω , we find that they have expansions

$$\tau = \sum_{I \in \{1,2\}^N} \tau_I, \quad \tau_I := \mu_I e^{\vartheta_I}, \quad F = \sum_{I \in \{1,2\}^N} M_I e^{\vartheta_I},$$

where μ_I are constants, M_I constant matrices, and

$$\vartheta_I = \sum_{k=1}^N \vartheta(p_k a_k) \quad I = (a_1, \dots, a_N), \quad a_k \in \{1, 2\}.$$

Recall that $p_{k,1} = p_k$ and $p_{k,2} = q_k$, $k = 1, \dots, N$. We have

$$\phi = \frac{F}{\tau}.$$

Since $\tau_{I,x} = p_I \tau_I$, where $p_I = p_{1,a_1} + \dots + p_{N,a_N}$ if $I = (a_1, \dots, a_N)$, we obtain

$$u = \frac{1}{\tau^2} \sum_{I,J \in \{1,2\}^N} (p_I - p_J)(\mu_J M_I - \mu_I M_J) e^{\vartheta_I + \vartheta_J}.$$

Note that (cf. [8])

$$\text{tr}(K M_I) = \left(p_I - \sum_{i=1}^N q_i \right) \mu_I,$$

so that

$$\text{tr}(K u) = 2(\log \tau)_{xx},$$

in accordance with (2.14).

If $\tau \neq 0$ and if $\mu_I > 0$ for all I with $\mu_I \neq 0$ in the expression for τ , regularity of the solution is guaranteed. Let

$$\mathcal{U}_I = \{(x, t) \in \mathbb{R}^2 \mid \log \tau_I \geq \log \tau_J, J \in \{1, 2\}^N\}.$$

We call this the region where ϑ_I dominates. As intersection of half-spaces, it is convex.

If $\mu_I > 0$, the tropical limit of ϕ in \mathcal{U}_I is³

$$\phi_I := \frac{M_I}{\mu_I}.$$

For $I \neq J$, the intersection $\mathcal{U}_I \cap \mathcal{U}_J$ is a segment of the straight line determined by $\log \tau_I = \log \tau_J$. On such a (visible) segment the value of u is given by

$$u_{IJ} = \frac{1}{2}(p_I - p_J)(\phi_I - \phi_J).$$

We find $\text{tr}(K u_{IJ}) = \frac{1}{2}(p_I - p_J)^2$ and introduce normalized values

$$\hat{u}_{IJ} = \frac{\phi_I - \phi_J}{p_I - p_J},$$

which satisfy $\text{tr}(K \hat{u}_{IJ}) = 1$. Using the notation

$$I_k(a) = (a_1, \dots, a_{k-1}, a, a_{k+1}, \dots, a_N),$$

³Appendix D in [16] explains the relation with the tropical limit defined via the Maslov dequantization formula.

the k -th soliton appears in space-time on segments of the straight lines determined by $\log \tau_{I_k(1)} = \log \tau_{I_k(2)}$, i.e.,

$$x + (p_k + q_k)t + \frac{1}{p_k - q_k} \log \frac{\mu_{I_k(1)}}{\mu_{I_k(2)}} = 0. \quad (3.7)$$

This also determines the asymptotic structure of a tropical limit graph of a pure N -soliton solution. Without restriction of generality, we can order the parameters such that $p_1 + q_1 < p_2 + q_2 < \dots < p_N + q_N$.⁴ If we represent p_i and q_i by the first two roots in (3.4), then $p_i + q_i$ is a strictly increasing function of $|\lambda|$, hence this order is obtained by choosing $0 < \lambda_1 < \lambda_2 < \dots < \lambda_N$. Now it follows from (3.7) that, for $t \ll 0$, the solitons appear along the x -axis according to their numbering, and for $t \gg 0$ they appear in reverse order. To the left of the center is the dominating phase region $\mathcal{U}_{1,\dots,1}$. Then follows counterclockwise $\mathcal{U}_{2,1,\dots,1}$, $\mathcal{U}_{2,2,1,\dots,1}$, ..., unless we get to the region $\mathcal{U}_{2,\dots,2}$ on the right hand side. Correspondingly, starting again from $\mathcal{U}_{1,\dots,1}$, we get clockwise to the regions $\mathcal{U}_{1,\dots,2}$, $\mathcal{U}_{1,\dots,2,2}$, ..., until we arrive at $\mathcal{U}_{2,\dots,2}$. These regions always appear in a tropical limit graph of a pure N -soliton solution. The remaining \mathcal{U}_I can only appear as *bounded* regions. But some may be empty. This depends on the value of higher Boussinesq hierarchy variables, also see Fig. 5 below.

Remark 3.1. It can happen that $\mu_I = 0$ for some multi-index I , so that e^{θ_I} is absent in the expression for τ , but that this exponential appears in the numerator of the expression for u , i.e., $M_I \neq 0$. Then some components of u will exhibit exponential growth in the region where this phase dominates, and a tropical limit does not exist.

3.2.1 Single soliton solution

For the 1-soliton solution we find

$$\tau = e^{px+p^2t+\varphi_0} + e^{qx+q^2t-\varphi_0}, \quad \varphi_0 = \frac{1}{2} \log(\eta K \xi),$$

assuming $\eta K \xi > 0$, and

$$\phi = (p - q) \frac{e^{px+p^2t+\varphi_0}}{e^{px+p^2t+\varphi_0} + e^{qx+q^2t-\varphi_0}} \frac{\xi \otimes \eta}{\eta K \xi}.$$

This yields

$$u = \frac{1}{2}(p - q)^2 \operatorname{sech}^2 \left(\frac{1}{2}(p - q)(x + (p + q)t) + \varphi_0 \right) \frac{\xi \otimes \eta}{\eta K \xi}.$$

Setting

$$p = -\sqrt{\beta} \frac{1 + 6\lambda - 3\lambda^2}{1 + 3\lambda^2}, \quad q = -\sqrt{\beta} \frac{1 - 6\lambda - 3\lambda^2}{1 + 3\lambda^2},$$

it takes the form

$$u = 4\beta \frac{18\lambda^2}{(1 + 3\lambda^2)^2} \operatorname{sech}^2 \left(2\sqrt{\beta} \frac{3\lambda}{1 + 3\lambda^2} \left(x - 2\sqrt{\beta} \frac{1 - 3\lambda^2}{1 + 3\lambda^2} t \right) + \varphi_0 \right) \frac{\xi \otimes \eta}{\eta K \xi}.$$

Via the symmetries (3.5), 1-soliton solutions with other choices of the roots are obtained from the above solution. If $\lambda^2 < 1/3$, the soliton moves from left to right. If $\lambda^2 > 1/3$, it moves from right

⁴With the chosen parametrization, $p_i + q_i = p_j + q_j$, for some i, j , implies either $p_i = p_j$ and $q_i = q_j$, or $p_i = q_j$ and $p_j = q_i$. We exclude these cases.

to left. For $\lambda^2 = 1/3$, it is stationary. In all cases, the absolute value of the velocity is less than $2\sqrt{\beta}$. We also note that $0 \leq \text{tr}(Ku) \leq 6\beta$.

The tropical limit graph of the 1-soliton solution is the boundary between the two dominating phase regions \mathcal{U}_1 and \mathcal{U}_2 . It is the straight line in space-time (xt -plane), determined by

$$x + (p + q)t + \frac{1}{p - q} \log(\eta K \xi) = 0,$$

with slope $-1/(p + q)$. We have

$$u_{1,2} = \frac{1}{2}(p - q)^2 \frac{\xi \otimes \eta}{\eta K \xi}, \quad \hat{u}_{1,2} = \frac{\xi \otimes \eta}{\eta K \xi}.$$

3.2.2 2-soliton solution

In this case ($N = 2$), we find

$$\tau = \alpha e^{\vartheta(p_1) + \vartheta(p_2)} + \kappa_{1,1} e^{\vartheta(p_1) + \vartheta(q_2)} + \kappa_{2,2} e^{\vartheta(p_2) + \vartheta(q_1)} + e^{\vartheta(q_1) + \vartheta(q_2)},$$

where

$$\begin{aligned} \kappa_{ij} &= \eta_i K \xi_j, \\ \alpha &= \kappa_{1,1} \kappa_{2,2} - \frac{(q_1 - p_1)(q_2 - p_2)}{(q_1 - p_2)(q_2 - p_1)} \kappa_{1,2} \kappa_{2,1}, \end{aligned} \tag{3.8}$$

and

$$\begin{aligned} F &= (q_1 - p_1)(q_2 - p_2) \left(\frac{\kappa_{2,2}}{p_2 - q_2} \xi_1 \otimes \eta_1 + \frac{\kappa_{1,1}}{p_1 - q_1} \xi_2 \otimes \eta_2 + \frac{\kappa_{1,2}}{q_1 - p_2} \xi_1 \otimes \eta_2 \right. \\ &\quad \left. + \frac{\kappa_{2,1}}{q_2 - p_1} \xi_2 \otimes \eta_1 \right) e^{\vartheta(p_1) + \vartheta(p_2)} + (p_1 - q_1) \xi_1 \otimes \eta_1 e^{\vartheta(p_1) + \vartheta(q_2)} + (p_2 - q_2) \xi_2 \otimes \eta_2 e^{\vartheta(p_2) + \vartheta(q_1)}. \end{aligned}$$

Hence, if $\alpha, \kappa_{1,1}, \kappa_{2,2} \neq 0$,

$$\begin{aligned} \phi_{1,1} &= \frac{(q_1 - p_1)(q_2 - p_2)}{\alpha} \left(\frac{\kappa_{2,2}}{p_2 - q_2} \xi_1 \otimes \eta_1 + \frac{\kappa_{1,2}}{q_1 - p_2} \xi_1 \otimes \eta_2 + \frac{\kappa_{2,1}}{q_2 - p_1} \xi_2 \otimes \eta_1 + \frac{\kappa_{1,1}}{p_1 - q_1} \xi_2 \otimes \eta_2 \right), \\ \phi_{1,2} &= \frac{p_1 - q_1}{\kappa_{1,1}} \xi_1 \otimes \eta_1, \quad \phi_{2,1} = \frac{p_2 - q_2}{\kappa_{2,2}} \xi_2 \otimes \eta_2, \quad \phi_{2,2} = 0. \end{aligned}$$

Choosing

$$p_i = -\sqrt{\beta} \frac{1 + 6\lambda_i - 3\lambda_i^2}{1 + 3\lambda_i^2}, \quad q_i = -\sqrt{\beta} \frac{1 - 6\lambda_i - 3\lambda_i^2}{1 + 3\lambda_i^2}, \tag{3.9}$$

we obtain via $\phi = F/\tau$ a 2-soliton solution of the potential BsQ_K equation.⁵ Fig. 2 shows examples of corresponding tropical limit graphs. Applying the symmetries (3.5), 2-soliton solutions with other choices of the roots are obtained from the above solution.

Furthermore, we find

$$\hat{u}_{11,12} = \frac{1}{\alpha} \left(\frac{\kappa_{1,2} \kappa_{2,1}}{\kappa_{1,1}} \frac{(p_1 - q_1)^2}{(p_1 - q_2)(p_2 - q_1)} \xi_1 \otimes \eta_1 - \kappa_{1,2} \frac{p_1 - q_1}{p_2 - q_1} \xi_1 \otimes \eta_2 \right)$$

⁵If $\alpha, \kappa_{1,1}$ or $\kappa_{2,2}$ vanishes, the tropical limit may still be defined. But since the corresponding phase is absent in τ , there is then no value $\phi_{1,1}, \phi_{1,2}$, respectively $\phi_{2,1}$.

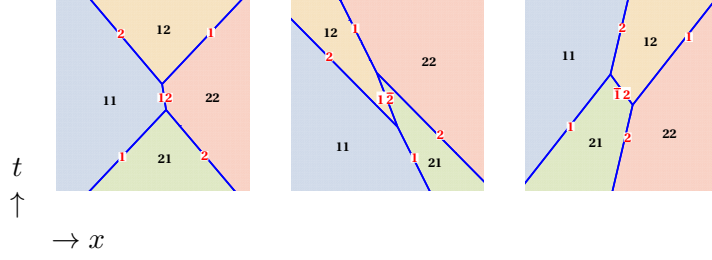


Figure 2: Tropical limit graphs of 2-soliton solutions of the $m = 2$ vector (i.e., $n = 1$) Bs q_K equation in space-time (xt -plane). Here we chose $K = (1, 1)$, $\eta_1 = \eta_2 = 1$, $\xi_1 = (1, 0)^T$, $\xi_2 = (0, 1)^T$, and the parameter values $(\lambda_1, \lambda_2) = (1/10, 2), (7/10, 4), (1/5, 5/11)$. This covers all possible directions of motion and interactions of two solitons. In the first case, the two solitons, numbered by 1 and 2, are moving towards each other (head-on collision), then form an intermediate “virtual” soliton (cf. [17, 7]), here denoted as a “composite” 12, which finally splits. This has no counterpart in the KdV case. In the other cases, the numbering of the virtual soliton draws on a formal analogy with particles and anti-particles (the latter indicated by a bar over the respective number).

$$\begin{aligned}
& -\kappa_{2,1} \frac{(p_1 - q_1)(p_2 - q_1)}{(p_1 - q_2)(p_2 - q_1)} \xi_2 \otimes \eta_1 + \kappa_{1,1} \xi_2 \otimes \eta_2 \Big), \\
\hat{u}_{11,21} &= \frac{1}{\alpha} \left(\kappa_{2,2} \xi_1 \otimes \eta_1 - \kappa_{1,2} \frac{p_2 - q_2}{p_2 - q_1} \xi_1 \otimes \eta_2 - \kappa_{2,1} \frac{(p_2 - q_1)(p_2 - q_2)}{(p_1 - q_2)(p_2 - q_1)} \xi_2 \otimes \eta_1 \right. \\
& \left. + \frac{\kappa_{1,2} \kappa_{2,1}}{\kappa_{2,2}} \frac{(p_2 - q_2)^2}{(p_1 - q_2)(p_2 - q_1)} \xi_2 \otimes \eta_2 \right), \\
\hat{u}_{12,22} &= \frac{1}{\kappa_{1,1}} \xi_1 \otimes \eta_1, \quad \hat{u}_{21,22} = \frac{1}{\kappa_{2,2}} \xi_2 \otimes \eta_2.
\end{aligned}$$

The map $\mathcal{R} : (\hat{u}_{11,21}, \hat{u}_{21,22}) \mapsto (\hat{u}_{12,22}, \hat{u}_{11,12})$ is a nonlinear Yang-Baxter map, it satisfies the (quantum) Yang-Baxter equation

$$\mathcal{R}_{12} \circ \mathcal{R}_{13} \circ \mathcal{R}_{23} = \mathcal{R}_{23} \circ \mathcal{R}_{13} \circ \mathcal{R}_{12}. \quad (3.10)$$

This map is also obtained from that of the KP theory, see Section 5 in [8], with the parameters restricted by (3.9). The fact that \mathcal{R} satisfies the Yang-Baxter equation follows from the Yang-Baxter property of the more general KP_K Yang-Baxter map. Alternatively, it follows from the 3-soliton solution and the fact that the polarizations do not depend on the independent variables, including higher hierarchy variables, see Section 3.2.5.

In the vector case, we obtain a *linear* map,

$$(\hat{u}_{12,22}, \hat{u}_{11,12}) = (\hat{u}_{11,21}, \hat{u}_{21,22}) R(\lambda_1, \lambda_2),$$

where

$$R(\lambda_i, \lambda_j) = \begin{pmatrix} \frac{\lambda_i - \lambda_j}{\lambda_i + \lambda_j} \frac{1 - \lambda_i - \lambda_j - 3\lambda_i \lambda_j}{1 - \lambda_i + \lambda_j + 3\lambda_i \lambda_j} & \frac{2\lambda_i}{\lambda_i + \lambda_j} \frac{1 + 3\lambda_j^2}{1 - \lambda_i + \lambda_j + 3\lambda_i \lambda_j} \\ \frac{2\lambda_j}{\lambda_i + \lambda_j} \frac{1 + 3\lambda_i^2}{1 - \lambda_i + \lambda_j + 3\lambda_i \lambda_j} & \frac{\lambda_j - \lambda_i}{\lambda_i + \lambda_j} \frac{1 + \lambda_i + \lambda_j - 3\lambda_i \lambda_j}{1 - \lambda_i + \lambda_j + 3\lambda_i \lambda_j} \end{pmatrix}.$$

Remark 3.2. Dropping the exponential factor in (3.6), which has only been introduced to achieve a convenient numbering of phases, in the $N = 2$ case we obtain

$$\tilde{\tau} = 1 + e^{\zeta_1} + e^{\zeta_2} + \left(\frac{\kappa_{1,1} \kappa_{2,2} - \kappa_{1,2} \kappa_{2,1}}{\kappa_{1,1} \kappa_{2,2}} + \frac{\kappa_{1,2} \kappa_{2,1}}{\kappa_{1,1} \kappa_{2,2}} \frac{(p_1 - p_2)(q_1 - q_2)}{(p_1 - q_2)(q_1 - p_2)} \right) e^{\zeta_1 + \zeta_2},$$

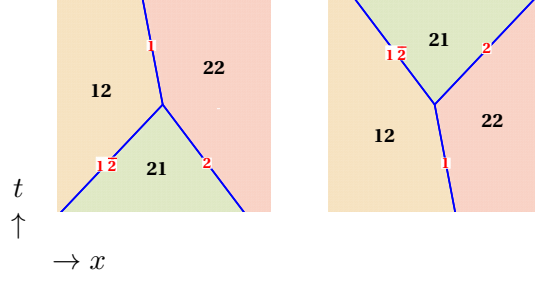


Figure 3: Tropical limit graphs of degenerate 2-soliton solutions of the $m = 2$ vector (i.e., $n = 1$) Bsq $_K$ equation. Here we chose $K = (1, 1)$, $\eta_1 = \eta_2 = 1$, $\xi_1 = (1, 0)^T$, $\xi_2 = (0, 1)^T$, and the parameter values $(\lambda_1, \lambda_2) = (7/10, 17/11)$ (so that $q_2 = q_1$), respectively $(\lambda_1, \lambda_2) = (7/10, 3/31)$ (so that $p_2 = p_1$).

where $\zeta_i = \vartheta(p_i) - \vartheta(q_i) + \log \kappa_{ii}$, assuming $\kappa_{ii} > 0$. Comparison with a known expression for the τ -function of the 2-soliton solution of the scalar Boussinesq (or KP) equation shows that this determines a solution of the scalar Boussinesq equation if $\kappa_{1,1}\kappa_{2,2} = \kappa_{1,2}\kappa_{2,1}$. We also note that, if $\kappa_{1,2}\kappa_{2,1} = 0$, the above expression factorizes to $\tilde{\tau} = (1 + e^{\zeta_1})(1 + e^{\zeta_2})$. In this case, the tropical limit graph is simply the superimposition of those of the factors⁶, hence there is no phase shift.

3.2.3 Degenerations of the pure 2-soliton solution of the vector Boussinesq equation

We consider the special cases where $p_1 = p_2$ or $q_1 = q_2$. Then we have $c_1 = c_2$, so that all parameters are roots of a single cubic equation. Since we represent p_i and q_i by the first two roots in (3.4), this means that $\lambda_2 = (1 - \lambda_1)/(3\lambda_1 + 1)$, respectively $\lambda_2 = (1 + \lambda_1)/(3\lambda_1 - 1)$. In both cases we have $\alpha = \kappa_{1,1}\kappa_{2,2} - \kappa_{1,2}\kappa_{2,1}$, which vanishes when we address the vector Boussinesq equation. If $q_2 = q_1$, we obtain

$$\tau = \left(e^{\vartheta(q_1)} + \kappa_{1,1} e^{\vartheta(p_1)} + \kappa_{2,2} e^{\vartheta(p_2)} \right) e^{\vartheta(q_1)}.$$

The factor $e^{\vartheta(q_1)}$ does not influence the tropical limit graph, which is shown in Fig. 3. If $p_2 = p_1$, we find

$$\tau = \left(e^{-\vartheta(p_1)} + \kappa_{1,1} e^{-\vartheta(q_1)} + \kappa_{2,2} e^{-\vartheta(q_2)} \right) e^{\vartheta(p_1) + \vartheta(q_1) + \vartheta(q_2)}.$$

The corresponding tropical limit graphs are Y-shaped (a soliton splits into two), respectively reverse Y-shaped (two solitons merge), see Fig. 3. Approaching such a solution by letting $q_2 \rightarrow q_1$, respectively $p_2 \rightarrow p_1$, in the 2-soliton solution in Section 3.2.2, we see that the edge representing the virtual soliton (cf. the second and third graph in Fig. 2) gets longer and longer, in such a way that the dominating phase region $\mathcal{U}_{1,1}$ finally disappears at infinity.

In these cases the R -matrix reduces to

$$R\left(\lambda, \frac{1 - \lambda}{3\lambda + 1}\right) = \begin{pmatrix} 0 & \frac{4\lambda}{(1-\lambda)(3\lambda+1)} \\ 1 & \frac{(1+\lambda)(3\lambda-1)}{(\lambda-1)(3\lambda+1)} \end{pmatrix},$$

respectively

$$R\left(\lambda, \frac{1 + \lambda}{3\lambda - 1}\right) = \begin{pmatrix} \frac{(1-\lambda)(1+3\lambda)}{4\lambda} & 1 \\ \frac{(1+\lambda)(3\lambda-1)}{4\lambda} & 0 \end{pmatrix}.$$

⁶This is evident from the Maslov dequantization formula, cf. Appendix D in [16], for example.

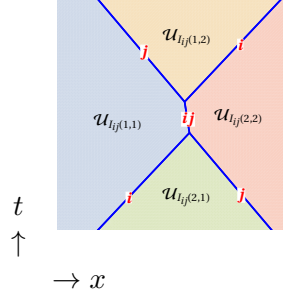


Figure 4: A 2-soliton part of an N -soliton tropical limit graph.

3.2.4 N -soliton solutions and phase shifts

If $I = (a_1, \dots, a_N)$ and $i < j$, let

$$I_{ij}(a, b) = (a_1, \dots, a_{i-1}, a, a_{i+1}, \dots, a_{j-1}, b, a_{j+1}, \dots, a_N).$$

The tropical limit graph of an N -soliton solution generically contains subgraphs describing 2-soliton interactions, see Fig. 4. In the vicinity of such a local 2-soliton interaction, the solution is well approximated by only keeping the four relevant phases (since exponentials of the others are then negligible) in the function τ . Hence

$$\tau \approx \tau_{ij}^I := \sum_{a,b=1,2} \tau_{I_{ij}(a,b)}, \quad \phi \approx \phi_{ij}^I := \frac{1}{\tau_{ij}^I} \sum_{a,b=1,2} \phi_{I_{ij}(a,b)} \tau_{I_{ij}(a,b)}.$$

Also see, e.g., [18] (Section 5 therein) for such approximations in the case of KP solitons.

The two parallel line segments corresponding to the path of the i -th soliton are determined by

$$x_{i,in} = -(p_i + q_i)t - (p_i - q_i)^{-1} \log \left(\frac{\mu_{I_{ij}(1,1)}}{\mu_{I_{ij}(2,1)}} \right), \quad x_{i,out} = -(p_i + q_i)t - (p_i - q_i)^{-1} \log \left(\frac{\mu_{I_{ij}(1,2)}}{\mu_{I_{ij}(2,2)}} \right).$$

Their shift along the x -axis, caused by the interaction with the j -th soliton, is

$$\delta_{ij}^I x := x_{i,out} - x_{i,in} = (p_i - q_i)^{-1} \log(A_{I_{ij}}), \quad A_{I_{ij}} = \frac{\mu_{I_{ij}(1,1)} \mu_{I_{ij}(2,2)}}{\mu_{I_{ij}(1,2)} \mu_{I_{ij}(2,1)}}.$$

The parallel line segments of the j -th soliton are given by

$$x_{j,in} = -(p_j + q_j)t - (p_j - q_j)^{-1} \log \left(\frac{\mu_{I_{ij}(2,1)}}{\mu_{I_{ij}(2,2)}} \right), \quad x_{j,out} = -(p_j + q_j)t - (p_j - q_j)^{-1} \log \left(\frac{\mu_{I_{ij}(1,1)}}{\mu_{I_{ij}(1,2)}} \right).$$

Their shift along the x -axis, caused by the interaction with the i -th soliton, is

$$\delta_{ji}^I x := x_{j,out} - x_{j,in} = -(p_j - q_j)^{-1} \log(A_{I_{ij}}).$$

If $N = 2$, we have $A_{I_{1,2}} = \alpha / (\kappa_{1,1} \kappa_{2,2})$ (also see [17] for the scalar case).

3.2.5 3-soliton solutions

If $N = 3$, we find

$$\tau = \gamma e^{\vartheta_{1,1,1}} + \alpha_{1,2} e^{\vartheta_{1,1,2}} + \alpha_{1,3} e^{\vartheta_{1,2,1}} + \alpha_{2,3} e^{\vartheta_{2,1,1}}$$

$$+\kappa_{1,1} e^{\vartheta_{1,2,2}} + \kappa_{2,2} e^{\vartheta_{2,1,2}} + \kappa_{3,3} e^{\vartheta_{2,2,1}} + e^{\vartheta_{2,2,2}},$$

where κ_{ij} , $i, j = 1, 2, 3$, are defined as in (3.8), and

$$\begin{aligned} \alpha_{ij} &= \kappa_{ii}\kappa_{jj} - \frac{(p_i - q_i)(p_j - q_j)}{(p_j - q_i)(p_i - q_j)} \kappa_{ij}\kappa_{ji}, \\ \gamma &= \kappa_{1,1}\kappa_{2,2}\kappa_{3,3} + \frac{(p_1 - q_1)(p_3 - q_3)(p_2 - q_2)}{(p_2 - q_1)(p_3 - q_2)(p_1 - q_3)} \kappa_{1,2}\kappa_{2,3}\kappa_{3,1} \\ &\quad + \frac{(p_1 - q_1)(p_3 - q_3)(p_2 - q_2)}{(p_3 - q_1)(p_1 - q_2)(p_2 - q_3)} \kappa_{1,3}\kappa_{2,1}\kappa_{3,2} - \frac{(p_1 - q_1)(p_2 - q_2)}{(p_2 - q_1)(p_1 - q_2)} \kappa_{1,2}\kappa_{2,1}\kappa_{3,3} \\ &\quad - \frac{(p_3 - q_3)(p_2 - q_2)}{(p_3 - q_2)(p_2 - q_3)} \kappa_{1,1}\kappa_{2,3}\kappa_{3,2} - \frac{(p_1 - q_1)(p_3 - q_3)}{(p_3 - q_1)(p_1 - q_3)} \kappa_{1,3}\kappa_{2,2}\kappa_{3,1}. \end{aligned}$$

Furthermore, if all coefficients of exponentials in τ are positive, we have the following tropical values of ϕ ,

$$\begin{aligned} \phi_{1,1,1} &= \frac{\kappa_{1,1}\kappa_{2,2}\kappa_{3,3}}{\gamma} \left(\tilde{\alpha}_{1,2}(p_3 - q_3) \xi_3 \otimes \eta_3 + \tilde{\alpha}_{1,3}(p_2 - q_2) \xi_2 \otimes \eta_2 + \tilde{\alpha}_{2,3}(p_1 - q_1) \xi_1 \otimes \eta_1 \right. \\ &\quad + (1 - \tilde{\alpha}_{2,3})\tilde{\alpha}_{1,2,3}(q_3 - p_2) \frac{\xi_2 \otimes \eta_3}{\kappa_{3,2}} + (1 - \tilde{\alpha}_{2,3})\tilde{\alpha}_{1,3,2}(q_2 - p_3) \frac{\xi_3 \otimes \eta_2}{\kappa_{2,3}} \\ &\quad + (1 - \tilde{\alpha}_{1,3})\tilde{\alpha}_{2,1,3}(q_3 - p_1) \frac{\xi_1 \otimes \eta_3}{\kappa_{3,1}} + (1 - \tilde{\alpha}_{1,3})\tilde{\alpha}_{2,3,1}(q_1 - p_3) \frac{\xi_3 \otimes \eta_1}{\kappa_{1,3}} \\ &\quad \left. + (1 - \tilde{\alpha}_{1,2})\tilde{\alpha}_{3,1,2}(q_2 - p_1) \frac{\xi_1 \otimes \eta_2}{\kappa_{2,1}} + (1 - \tilde{\alpha}_{1,2})\tilde{\alpha}_{3,2,1}(q_1 - p_2) \frac{\xi_2 \otimes \eta_1}{\kappa_{1,2}} \right), \\ \phi_{1,1,2} &= \frac{1}{\tilde{\alpha}_{1,2}} \left((p_1 - q_1) \frac{\xi_1 \otimes \eta_1}{\kappa_{1,1}} + (p_2 - q_2) \frac{\xi_2 \otimes \eta_2}{\kappa_{2,2}} + (q_2 - p_1)(1 - \tilde{\alpha}_{1,2}) \frac{\xi_1 \otimes \eta_2}{\kappa_{2,1}} \right. \\ &\quad \left. + (q_1 - p_2)(1 - \tilde{\alpha}_{1,2}) \frac{\xi_2 \otimes \eta_1}{\kappa_{1,2}} \right), \\ \phi_{1,2,1} &= \frac{1}{\tilde{\alpha}_{1,3}} \left((p_1 - q_1) \frac{\xi_1 \otimes \eta_1}{\kappa_{1,1}} + (p_3 - q_3) \frac{\xi_3 \otimes \eta_3}{\kappa_{3,3}} + (q_3 - p_1)(1 - \tilde{\alpha}_{1,3}) \frac{\xi_1 \otimes \eta_3}{\kappa_{3,1}} \right. \\ &\quad \left. + (q_1 - p_3)((1 - \tilde{\alpha}_{1,3}) \frac{\xi_3 \otimes \eta_1}{\kappa_{1,3}}) \right), \\ \phi_{2,1,1} &= \frac{1}{\tilde{\alpha}_{2,3}} \left((p_2 - q_2) \frac{\xi_2 \otimes \eta_2}{\kappa_{2,2}} + (p_3 - q_3) \frac{\xi_3 \otimes \eta_3}{\kappa_{3,3}} + (q_3 - p_2)(1 - \tilde{\alpha}_{2,3}) \frac{\xi_2 \otimes \eta_3}{\kappa_{3,2}} \right. \\ &\quad \left. + (q_2 - p_3)(1 - \tilde{\alpha}_{2,3}) \frac{\xi_3 \otimes \eta_2}{\kappa_{2,3}} \right), \\ \phi_{1,2,2} &= (p_1 - q_1) \frac{\xi_1 \otimes \eta_1}{\kappa_{1,1}}, \quad \phi_{2,1,2} = (p_2 - q_2) \frac{\xi_2 \otimes \eta_2}{\kappa_{2,2}}, \\ \phi_{2,2,1} &= (p_3 - q_3) \frac{\xi_3 \otimes \eta_3}{\kappa_{3,3}}, \quad \phi_{2,2,2} = 0, \end{aligned}$$

where

$$\tilde{\alpha}_{ij} = 1 - \frac{(p_i - q_i)(p_j - q_j) \kappa_{ij}\kappa_{ji}}{(p_j - q_i)(p_i - q_j) \kappa_{ii}\kappa_{jj}}, \quad \tilde{\alpha}_{kij} = 1 - \frac{(p_k - q_k)(p_j - q_i) \kappa_{ik}\kappa_{kj}}{(p_k - q_i)(p_j - q_k) \kappa_{kk}\kappa_{ij}}.$$

Examples of corresponding tropical limit graphs are shown in Fig. 5. Here we extended the phase expression (2.7) by including the next hierarchy variable:

$$\vartheta(P) = Px + P^2t + P^4s.$$

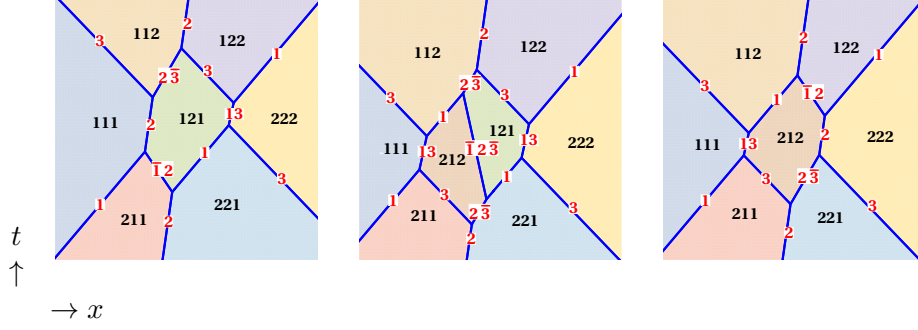


Figure 5: Tropical limit graphs of 3-soliton solutions of the $m = 3$ vector ($n = 1$) Bs q_K equation with $K = (1, 1, 1)$, $\eta_i = 1$, $i = 1, 2, 3$, $\xi_1 = (1, 0, 0)^T$, $\xi_2 = (0, 1, 0)^T$, $\xi_3 = (0, 0, 1)^T$, and p_i, q_i are given by (3.9) with $(\lambda_1, \lambda_2, \lambda_3) = (1/6, 1/2, 4)$. The three graphs correspond to consecutive values of the next hierarchy variable, $s = -50, 10, 50$. According to the general asymptotic structure of pure soliton solutions, $\mathcal{U}_{1,2,1}$ and $\mathcal{U}_{2,1,2}$ are the only possible interior regions.

The first and the third graph correspond to a large negative, respectively large positive value of s . The sequences of 2-soliton interactions are according to the left, respectively right hand side of the Yang-Baxter equation. Since the polarizations along edges of a tropical limit graph do not depend on the variables (x, t, s) , we conclude that the Yang-Baxter equation holds.

3.3 Other soliton configurations

Now we consider solutions involving three roots of the cubic equation. There are then two cases, either

$$\theta = \theta_1 e^{\vartheta(P_1)} + \theta_2 e^{\vartheta(P_2)}, \quad \chi = e^{-\vartheta(P_3)} \chi_3,$$

or

$$\theta = \theta_3 e^{\vartheta(P_3)}, \quad \chi = e^{-\vartheta(P_1)} \chi_1 + e^{-\vartheta(P_2)} \chi_2.$$

The second, “dual” choice can be obtained from the first by applying the symmetry $\phi \mapsto \phi^T$, $t \mapsto -t$, and using $\chi_a \leftrightarrow \theta_a^T$, $P_a \mapsto -P_a^T$. In the following we use again the decomposition (3.2), but with the rescaling $\xi_{ia} \mapsto (p_{i,3} - p_{ia}) \xi_{ia}$, $a = 1, 2$.

Example 3.3. We consider the simplest case, $N = 1$. Hence $i = 1$ in p_{ia} and ξ_{ia} . The corresponding index will now be suppressed. Then we have

$$\theta = (p_3 - p_1) \xi_1 e^{\vartheta(p_1)} + (p_3 - p_2) \xi_2 e^{\vartheta(p_2)}, \quad \chi = e^{-\vartheta(p_3)} \eta_3.$$

Here ξ_a , $a = 1, 2$, are m -component column vectors, η_3 is an n -component row vector. Then

$$\tau = e^{\vartheta(p_3)} \Omega = e^{\vartheta(p_3)} + \eta_3 K \xi_1 e^{\vartheta(p_1)} + \eta_3 K \xi_2 e^{\vartheta(p_2)}$$

and

$$\phi = -\frac{1}{\tau} \left((p_3 - p_1) \xi_1 \otimes \eta_3 e^{\vartheta(p_1)} + (p_3 - p_2) \xi_2 \otimes \eta_3 e^{\vartheta(p_2)} \right).$$

We set

$$p_1 = -\frac{\sqrt{\beta} (1 + 6\lambda - 3\lambda^2)}{1 + 3\lambda^2}, \quad p_2 = -\frac{\sqrt{\beta} (1 - 6\lambda - 3\lambda^2)}{1 + 3\lambda^2}, \quad p_3 = \frac{2\sqrt{\beta} (1 - 3\lambda^2)}{1 + 3\lambda^2}.$$

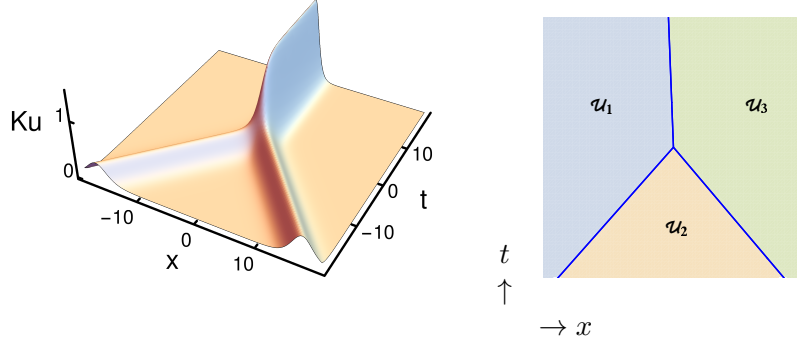


Figure 6: Merging of two $m = 2$ vector ($n = 1$) solitons into one, according to Example 3.3. Here we chose $K = (1, 1)$, $\theta_1 = (1, 0)^T$, $\theta_2 = (0, 1)^T$, $\eta_3 = 1$ and $\lambda = 1/7$.

The solution describes the merging of two solitons into a single one, also see Fig. 6. If $\lambda \in \{0, \pm 1/3, \pm 1\}$, two of the p_i are equal and the solution reduces to a 1-soliton solution. The dual case describes the splitting of a single soliton into two.

Remark 3.4. In contrast to the KdV reduction of KP, where a quadratic equation rules the game, Bsq_K thus admits solutions with a tropical limit graph in space-time having the most elementary rooted binary tree shape: three edges meeting at a vertex. We may speculate that in higher Gelfand-Dickey reductions there are corresponding limits for the number of edges forming a rooted binary tree.

Example 3.5. For $N = 2$ and $P_a = \text{diag}(p_{1,a}, p_{2,a})$, $a = 1, 2, 3$, we obtain

$$\phi = \frac{F}{\tau}$$

with

$$\begin{aligned} \tau &= e^{\vartheta(p_{1,3}) + \vartheta(p_{2,3})} \det(\Omega) \\ &= \sum_{a,b=1}^2 \alpha_{ab} e^{\tilde{\vartheta}_{ab}} + \kappa_{1,1,1} e^{\tilde{\vartheta}_{1,3}} + \kappa_{1,1,2} e^{\tilde{\vartheta}_{2,3}} + \kappa_{2,2,1} e^{\tilde{\vartheta}_{3,1}} + \kappa_{2,2,2} e^{\tilde{\vartheta}_{3,2}} + e^{\tilde{\vartheta}_{3,3}} \end{aligned}$$

and

$$\begin{aligned} F &= (p_{1,3} - p_{1,1})(p_{2,3} - p_{2,1}) \left(\frac{\kappa_{1,1,1} \xi_{2,1} \otimes \eta_2}{p_{1,1} - p_{1,3}} + \frac{\kappa_{1,2,1} \xi_{1,1} \otimes \eta_2}{p_{1,3} - p_{2,1}} + \frac{\kappa_{2,1,1} \xi_{2,1} \otimes \eta_1}{p_{2,3} - p_{1,1}} + \frac{\kappa_{2,2,1} \xi_{1,1} \otimes \eta_1}{p_{2,1} - p_{2,3}} \right) e^{\tilde{\vartheta}_{1,1}} \\ &+ (p_{1,3} - p_{1,2})(p_{2,3} - p_{2,1}) \left(\frac{\kappa_{1,1,2} \xi_{2,1} \otimes \eta_2}{p_{1,2} - p_{1,3}} + \frac{\kappa_{1,2,1} \xi_{1,2} \otimes \eta_2}{p_{1,3} - p_{2,1}} + \frac{\kappa_{2,1,2} \xi_{2,1} \otimes \eta_1}{p_{2,3} - p_{1,2}} + \frac{\kappa_{2,2,1} \xi_{1,2} \otimes \eta_1}{p_{2,1} - p_{2,3}} \right) e^{\tilde{\vartheta}_{2,1}} \\ &+ (p_{1,3} - p_{1,1})(p_{2,3} - p_{2,2}) \left(\frac{\kappa_{1,1,1} \xi_{2,2} \otimes \eta_2}{p_{1,1} - p_{1,3}} + \frac{\kappa_{1,2,2} \xi_{1,1} \otimes \eta_2}{p_{1,3} - p_{2,2}} + \frac{\kappa_{2,1,1} \xi_{2,2} \otimes \eta_1}{p_{2,3} - p_{1,1}} + \frac{\kappa_{2,2,2} \xi_{1,1} \otimes \eta_1}{p_{2,2} - p_{2,3}} \right) e^{\tilde{\vartheta}_{1,2}} \\ &+ (p_{1,3} - p_{1,2})(p_{2,3} - p_{2,2}) \left(\frac{\kappa_{1,1,2} \xi_{2,2} \otimes \eta_2}{p_{1,2} - p_{1,3}} + \frac{\kappa_{1,2,2} \xi_{1,2} \otimes \eta_2}{p_{1,3} - p_{2,2}} + \frac{\kappa_{2,1,2} \xi_{2,2} \otimes \eta_1}{p_{2,3} - p_{1,2}} + \frac{\kappa_{2,2,2} \xi_{1,2} \otimes \eta_1}{p_{2,2} - p_{2,3}} \right) e^{\tilde{\vartheta}_{2,2}} \\ &+ (p_{1,1} - p_{1,3}) \xi_{1,1} \otimes \eta_1 e^{\tilde{\vartheta}_{1,3}} + (p_{1,2} - p_{1,3}) \xi_{1,2} \otimes \eta_1 e^{\tilde{\vartheta}_{2,3}} + (p_{2,1} - p_{2,3}) \xi_{2,1} \otimes \eta_2 e^{\tilde{\vartheta}_{3,1}} \\ &+ (p_{2,2} - p_{2,3}) \xi_{2,2} \otimes \eta_2 e^{\tilde{\vartheta}_{3,2}}. \end{aligned}$$

Here we set

$$\tilde{\vartheta}_{ab} = \vartheta(p_{1,a}) + \vartheta(p_{2,b}) \quad a, b = 1, 2, 3,$$

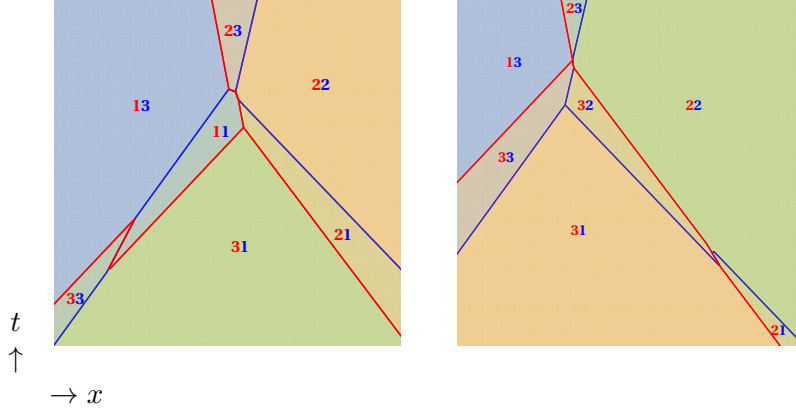


Figure 7: Tropical limit graphs of 2×2 Boussinesq solutions according to Example 3.6. In the first example, we set $\eta_1 = (10^2, 0)$, $\eta_2 = (0, 10^{-2})$, $\xi_{1,1} = (1, 1)^T$, $\xi_{1,2} = (1, 0)^T$, $\xi_{2,1} = (0, 1)^T$, $\xi_{2,2} = (1, 2)^T$. In the second we chose $\eta_1 = (10^{-4}, 0)$, $\eta_2 = (0, 10^4)$, $\xi_{1,1} = (1, 0)^T$, $\xi_{1,2} = (1, -2)^T$, $\xi_{2,1} = (2, 1)^T$, $\xi_{2,2} = (1, 1)^T$. Only seven of the nine phases appearing in the expression for τ are visible.

$$\begin{aligned} \kappa_{ija} &= \eta_i K \xi_{j,a} & i, j = 1, 2, \quad a = 1, 2, \\ \alpha_{ab} &= \kappa_{1,1,a} \kappa_{2,2,b} - \frac{(p_{1,a} - p_{1,3})(p_{2,b} - p_{2,3})}{(p_{1,a} - p_{2,3})(p_{2,b} - p_{1,3})} \kappa_{2,1,a} \kappa_{1,2,b} & a, b = 1, 2, \end{aligned}$$

using (3.2) with

$$\chi_3 = \begin{pmatrix} \eta_1 \\ \eta_2 \end{pmatrix}.$$

Example 3.6. According to Proposition 3.7 below, in the scalar and vector case there is no regular solution in the class given by Example 3.5, with all possible phases present in the expression for τ . But corresponding regular solutions exist, for example, in the 2×2 matrix case. Fig. 7 shows two examples of tropical limit graphs. Here we chose $K = \text{diag}(1, 1)$ and $\lambda_1 = 7/10$, $\lambda_2 = 4$.

3.3.1 Solutions of the vector Boussinesq equation

In this subsection we consider the case of the m -component vector ($n = 1$) Boussinesq equation. This includes the scalar Boussinesq case ($m = 1$).

$N = 2$.

Proposition 3.7. *For the vector Boussinesq equation, and with real parameters, it is not possible that all coefficients in the expression for τ in the $N = 2$ case (Example 3.5) are positive.*

Proof. In the vector case, where η_i are scalars, we have $\kappa_{2,1,a} \kappa_{1,2,b} = \kappa_{1,1,a} \kappa_{2,2,b}$, hence

$$\alpha_{ab} = \kappa_{1,1,a} \kappa_{2,2,b} \tilde{\alpha}_{ab}, \quad \tilde{\alpha}_{ab} := \frac{(p_{2,3} - p_{1,3})(p_{1,a} - p_{2,b})}{(p_{1,a} - p_{2,3})(p_{2,b} - p_{1,3})}. \quad (3.11)$$

Let us assume $\kappa_{iia} > 0$, $i = 1, 2$, $a = 1, 2$, and $\alpha_{ab} > 0$, $a, b = 1, 2$. This implies that, for $a = 1, 2$ and $b = 1, 2$, either

$$(p_{2,3} - p_{1,3})(p_{1,a} - p_{2,b}) > 0 \quad \text{and} \quad (p_{1,a} - p_{2,3})(p_{2,b} - p_{1,3}) > 0,$$

or

$$(p_{2,3} - p_{1,3})(p_{1,a} - p_{2,b}) < 0 \quad \text{and} \quad (p_{1,a} - p_{2,3})(p_{2,b} - p_{1,3}) < 0$$

holds. Next we observe that, for $i = 1, 2$, the solutions (3.4) of the cubic equation satisfy one of the following sets of inequalities (also see Fig. 1).

1. $p_{i,3} \leq -\sqrt{\beta} \leq p_{i,2} \leq \sqrt{\beta} < p_{i,1}$.
2. $p_{i,2} \leq -\sqrt{\beta} \leq p_{i,3} \leq \sqrt{\beta} \leq p_{i,1}$.
3. $p_{i,2} \leq -\sqrt{\beta} \leq p_{i,1} \leq \sqrt{\beta} \leq p_{i,3}$.

This leaves us with nine cases. In all of them, an analysis of the inequalities leads to a contradiction. \square

As a consequence of the above proposition, if all possible terms are present in the $N = 2$ function τ (Example 3.5), in the vector Boussinesq case the solution has a singularity. Regular solutions are then only possible if at least one of the coefficients of exponentials in τ vanishes. In order to achieve this, we have to choose special values of some parameters, or special relations between parameters.

To see what happens if one of the coefficients of exponentials in τ vanishes, let us consider the case where $K\xi_{1,2} = 0$ (other cases lead to the same conclusions). Then the $N = 2$ function τ reduces to

$$\begin{aligned} \tau &= \alpha_{1,1} e^{\tilde{\vartheta}_{1,1}} + \alpha_{1,2} e^{\tilde{\vartheta}_{1,2}} + \kappa_{1,1,1} e^{\tilde{\vartheta}_{1,3}} + \kappa_{2,2,1} e^{\tilde{\vartheta}_{3,1}} + \kappa_{2,2,2} e^{\tilde{\vartheta}_{3,2}} + e^{\tilde{\vartheta}_{3,3}} \\ &= e^{\vartheta(p_{1,3})} \left(e^{\vartheta(p_{2,3})} + K\xi_{2,1} e^{\vartheta(p_{2,1})} + K\xi_{2,2} e^{\vartheta(p_{2,2})} \right) \\ &\quad + K\xi_{1,1} e^{\vartheta(p_{1,1})} \left(e^{\vartheta(p_{2,3})} + \tilde{\alpha}_{1,1} K\xi_{2,1} e^{\vartheta(p_{2,1})} + \tilde{\alpha}_{1,2} K\xi_{2,2} e^{\vartheta(p_{2,2})} \right), \end{aligned} \quad (3.12)$$

where we set $\eta_i = 1$, which is no restriction of generality in the case under consideration, and $\tilde{\alpha}_{1,1}, \tilde{\alpha}_{1,2}$ are defined in (3.11). In the last expression in (3.12), the part in the first brackets corresponds to an $N = 1$ soliton configuration, cf. Example 3.3. If the part in the other brackets had the same coefficients, τ would factorize and we would obtain a tropical limit graph which is a superimposition of that of the $N = 1$ Y-shaped solution and a single soliton. Different coefficients lead to a deformation, introducing phase shifts. Fig. 8 shows an example.

The condition $K\xi_{1,2} = 0$ eliminates some phases from the function τ , i.e., we have $\mu_{ab} = 0$ for some a, b . If we choose $\xi_{1,2} = (1, -1)^T$, keeping otherwise the data specified in Fig. 8, then we still have $K\xi_{1,2} = 0$, but some M_{ab} is different from zero, although $\mu_{ab} = 0$.

The last proposition tells us that, however small (with respect to a suitable norm) we choose a neighborhood of such a regular solution, in the set of solutions, it contains singular solutions.

An $N > 2$ solution locally consists approximately of $N = 2$ solutions. We should thus expect the above proposition to extend to $N > 2$. But we will not attempt to provide a rigorous proof here. In the following we show that solutions with $N = 3$ exist, where the singularities only appear in a compact region of space-time.

$N = 3$. We set $P_a = \text{diag}(p_a, q_a, r_a)$, $a = 1, 2, 3$, and obtain

$$\tau = \sum_{a,b,c=1}^3 \mu_{abc} e^{\tilde{\vartheta}_{abc}} \quad (3.13)$$

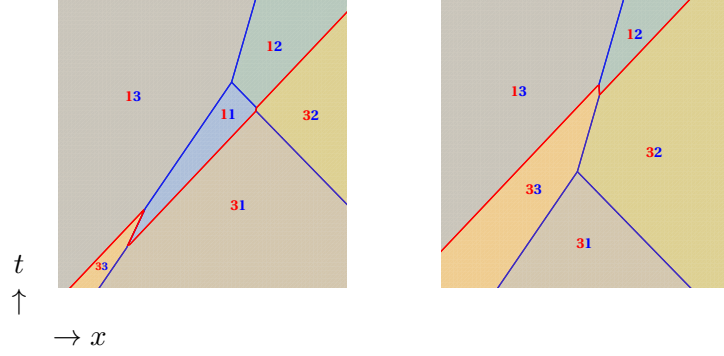


Figure 8: Tropical limit graph of a solution of the $m = 2$ vector ($n = 1$) Boussinesq equation from the class with τ given by (3.12). The solution represents a (nonlinear) superposition of a branching soliton (marked blue) and a single soliton (marked red). Here we chose $K = (1, 1)$, $\lambda_1 = 7/10$, $\lambda_2 = 5$, $\xi_{1,1} = (1, 0)^T$, $\xi_{1,2} = (0, 0)^T$, $\xi_{2,1} = (1, 1)^T$, $\xi_{2,2} = (2, 1)^T$ and $\eta_1 = 10^2$, $\eta_2 = 10^{-2}$, respectively $\eta_1 = 10^{-3}$, $\eta_2 = 10^{-3}$. The same graphs are obtained from a solution of the scalar Boussinesq equation, using $K = 1$ and $\xi_{1,1} = 1$, $\xi_{1,2} = 0$, $\xi_{2,1} = 2$, $\xi_{2,2} = 3$.

with $\tilde{\vartheta}_{abc} = \vartheta(p_a) + \vartheta(q_a) + \vartheta(r_a)$ and

$$\mu_{abc} = \frac{(p_3 - q_3)(p_3 - r_3)(q_3 - r_3)(p_a - q_b)(p_a - r_c)(q_b - r_c)}{(p_a - q_3)(p_a - r_3)(q_b - p_3)(q_b - r_3)(r_c - p_3)(r_c - q_3)} \frac{\eta_1 \eta_2 \eta_3 \kappa_{1,a} \kappa_{2,b} \kappa_{3,c}}{(-\eta_1 \kappa_{1,a})^{\delta_a^3} (-\eta_2 \kappa_{2,b})^{\delta_b^3} (-\eta_3 \kappa_{3,c})^{\delta_c^3}},$$

where δ_a^i is the Kronecker symbol. Furthermore,

$$\begin{aligned} \Phi_{abc} = & \frac{(p_a - p_3)(p_a - q_3)(p_a - r_3)}{(p_a - q_b)(p_a - r_c)} \frac{\xi_{1,a}}{\kappa_{1,a}} + \frac{(q_b - q_3)(q_b - p_3)(q_b - r_3)}{(q_b - p_a)(q_b - r_c)} \frac{\xi_{2,b}}{\kappa_{2,b}} \\ & + \frac{(r_c - r_3)(r_c - p_3)(r_c - q_3)}{(r_c - p_a)(r_c - q_b)} \frac{\xi_{3,c}}{\kappa_{3,c}}. \end{aligned}$$

If τ has also *negative* summands, strictly its tropical limit is not defined. Notwithstanding this, we can determine (and plot) the regions where the logarithm of the *absolute value* of a summand of τ dominates. On a boundary segment between such (generalized) dominating phase regions, where the corresponding summand in τ is positive for one and negative for the other, the soliton solution is singular. This is so because close to such a boundary segment contributions from all other summands are exponentially suppressed, hence negligible. Furthermore, singularities can only appear at such a boundary segment, since everywhere else either a single summand of τ dominates and all others are negligible, or we have a boundary segment along which two summands with the same sign have equal values and all other summands are negligible. The latter two cases exclude a singularity.

Fig. 9 shows an example of such a modified tropical limit graph. The white regions are dominated by phases having negative contributions to the τ -function. In these regions the solution is still regular, but on the interface between a “positive” and a “negative” phase region (plotted in red), and only there, the solution becomes singular. A similar solution of the scalar Boussinesq equation appeared in [5] (see Figure 8 therein).

4 The case $C' \neq -C$

We can use the transformations in Remark 2.2 to achieve that both, C and C' , have Jordan normal form. Then (2.13) generically implies $\Omega_0 = 0$. This will be assumed in the following. Choosing

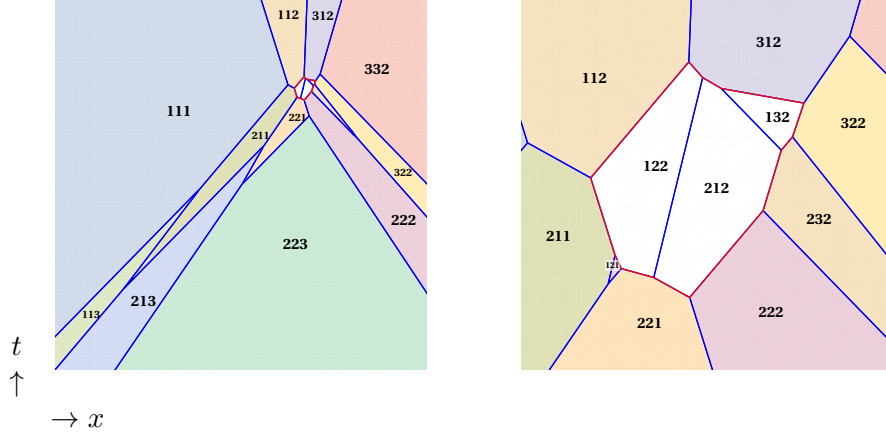


Figure 9: Modified tropical limit graph of a solution of the $m = 2$ vector ($n = 1$) Boussinesq equation from the class with τ given by (3.13). The second plot zooms into the region where most of the phases meet. There are 6 incoming and 3 outgoing solitons. The solution is singular only on the (red) boundary of the white region. Here we chose $K = (1, 1)$, $\lambda_1 = 1/6$, $\lambda_2 = 1/4$, $\xi_{1,1} = (-1/2, 0)^T$, $\xi_{2,1} = (1, -1/2)^T$, $\xi_{3,1} = (-3/2, -3/2)^T$, $\xi_{1,2} = (0, -1)^T$, $\xi_{2,2} = (-3/2, -1)^T$, $\xi_{3,2} = (3/2, -3)^T$, and $\eta_i = 1$ for $i = 1, 2, 3$. The phases $\vartheta_{3,1,1}$ and $\vartheta_{3,1,3}$ are nowhere dominant, hence do not appear in the tropical limit plot.

diagonal matrices

$$P_a = \text{diag}(p_{1,a}, \dots, p_{N,a}), \quad Q_a = \text{diag}(q_{1,a}, \dots, q_{N,a}), \\ C = \text{diag}(c_1, \dots, c_N), \quad C' = \text{diag}(c'_1, \dots, c'_N),$$

(2.8) and (2.10) require

$$p_{ia}^3 = 3\beta p_{ia} + c_i, \quad q_{ia}^3 = 3\beta q_{ia} - c'_i.$$

For each $i = 1, \dots, N$, we represent the roots p_{ia} , $a = 1, 2, 3$, of the first cubic equation as in (3.4), using a parameter λ_i . In the same way we represent the roots q_{ia} , $a = 1, 2, 3$, of the second cubic equation using a parameter ν_i . We assume that $p_{ia} \neq p_{jb}$ and $q_{ia} \neq q_{jb}$ for $i \neq j$ or $a \neq b$. Now we have

$$\theta = \sum_{a=1}^3 \theta_a e^{\vartheta(P_a)}, \quad \chi = \sum_{a=1}^3 e^{\vartheta(-Q_a)} \chi_a.$$

Assuming $q_{ib} \neq p_{ja}$ for all combinations of indices, from (2.11) and (2.12) we obtain

$$\Omega_{ij} = \sum_{a,b=1}^3 \frac{\eta_{ib} K \xi_{ja}}{q_{ib} - p_{ja}} e^{\vartheta(p_{ja}) - \vartheta(q_{ib})} \quad i, j = 1, \dots, N.$$

The BsQ_K solution is given by

$$\phi = \frac{F}{\tau},$$

where now

$$\tau = \det(\Omega) = \sum_{I, J \in \{1, 2, 3\}^N} \tau_{IJ}, \quad \tau_{IJ} = \mu_{IJ} e^{\vartheta_{IJ}}, \quad \vartheta_{IJ} = \sum_{i=1}^N \left(\vartheta(p_{ia_i}) - \vartheta(p_{ib_i}) \right),$$

$$F = -\theta \operatorname{adj}(\Omega) \chi =: \sum_{I, J \in \{1, 2, 3\}^N} \phi_{IJ} \tau_{IJ},$$

with constants μ_{IJ} and constant matrices ϕ_{IJ} , of a certain structure. Here $\operatorname{adj}(\Omega)$ denotes the adjugate of the matrix Ω , and we wrote $I = (a_1, \dots, a_N)$, $J = (b_1, \dots, b_N)$ in the expression for τ_{IJ} . If a phase ϑ_{IJ} is present in τ , and if the tropical limit exists, then the tropical value of ϕ in the corresponding dominating phase region is ϕ_{IJ} . We decompose θ_a and χ_a as in (3.2).

In the following we restrict our considerations to the case $N = 1$. Then Ω is a scalar, consisting of at most nine summands. We obtain $\phi = F/\tau$ with

$$\begin{aligned} \tau = \Omega &= \sum_{a, b=1}^3 \frac{\kappa_{ba}}{q_b - p_a} e^{\vartheta(p_a) - \vartheta(q_b)}, & \kappa_{ba} &= \chi_b K \theta_a, \\ F &= - \sum_{a, b=1}^3 \theta_a \otimes \chi_b e^{\vartheta(p_a) - \vartheta(q_b)}. \end{aligned}$$

Hence

$$\phi_{ab} = \frac{p_a - q_b}{\kappa_{ba}} \theta_a \otimes \chi_b.$$

In the scalar and vector Boussinesq case, one can show that there is no regular solution of the above form, with real parameters and with *all* coefficients of exponentials in τ different from zero. This means that, however small (using a suitable norm) we choose a neighborhood of such a regular solution, in the set of solutions, it contains singular solutions. The first statement is not true in the matrix case.

Example 4.1. Let $m = n = 3$, $K = \operatorname{diag}(1, 1, 1)$,

$$\begin{aligned} \chi_1 &= \begin{pmatrix} 1 & 0 & 0 \end{pmatrix}, & \chi_2 &= \begin{pmatrix} 0 & 1 & 0 \end{pmatrix}, & \chi_3 &= \begin{pmatrix} 0 & 0 & 1 \end{pmatrix}, \\ \theta_1 &= \begin{pmatrix} 1 \\ 1 \\ 1 \end{pmatrix}, & \theta_2 &= \begin{pmatrix} -2 \\ 1 \\ -1 \end{pmatrix}, & \theta_3 &= \begin{pmatrix} -1 \\ 1 \\ -1 \end{pmatrix}, \end{aligned}$$

and $\lambda_1 = 1/5$, $\nu_1 = 3/2$. The function τ , given above, is then a positive linear combination of nine independent exponentials, which is the maximal number. All nine phases, appearing in the corresponding function τ , are visible in the tropical limit graph, see Fig. 10. The three interior phase regions are hardly expected from the plot on the left hand side and reveal a complicated interaction pattern. Fig. 11 shows another, though simpler example, where the relation is evident.

5 Conclusions

The scalar Boussinesq equation exhibits richer soliton interactions than the KdV equation. This concerns head-on collisions and inelastic scattering. All this is nicely revealed in the tropical limit. Here the function τ determines the solution via $u = 2(\log \tau)_{xx}$.

In the vector case ($m = 1$ or $n = 1$), we have $\operatorname{tr}(Ku) = 2(\log \tau)_{xx}$, and this is a solution of the scalar Boussinesq equation. Specifying initial polarizations for sufficiently large negative time t , i.e., those of the incoming solitons, the distribution of polarizations over the tropical limit graph is obtained, for the class of solutions treated in Section 3, by use of a Yang-Baxter R -matrix. For a more general class of solutions, also a tetragon map is at work, cf. Section 8 in [9].

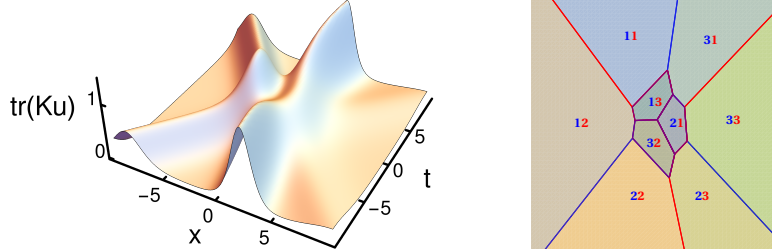


Figure 10: Plot of $\text{tr}(Ku) = 2(\log \tau)_{xx}$ and tropical limit graph the 3×3 matrix solution as specified in Example 4.1. This shows a 3-soliton solution where none of the outgoing solitons has a velocity equal to that of one of the incoming solitons. The tropical limit graph shows that this is actually a superposition of a splitting soliton (red Y-shaped) and two merging solitons (blue reversed Y-shaped graph).

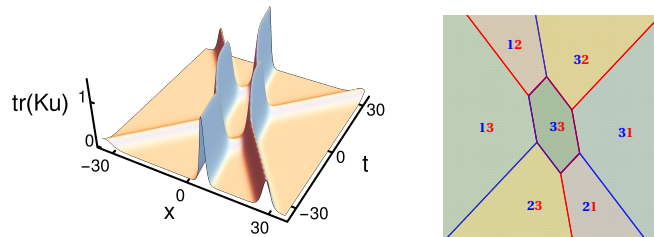


Figure 11: Plot of $\text{tr}(Ku) = 2(\log \tau)_{xx}$ and tropical limit graph of a 3×3 matrix solution, as given in Section 4, with $N = 1$ and $\theta_1 = (-1, 1, 1)^T$, $\theta_2 = (-2, 1, 1)$, $\theta_3 = (-1, -1, -1)$, $\lambda_1 = 1/10$, $\nu_1 = 1/10 + 10^{-5}$. Only seven of the nine phases, appearing in the corresponding function τ , are visible.

For the matrix ($m, n > 1$) Boussinesq equation, $\text{tr}(Ku) = 2(\log \tau)_{xx}$ is not in general a solution of the scalar equation. A *nonlinear* Yang-Baxter map is at work, which is a reduction of the corresponding matrix KP Yang-Baxter map, recently obtained in [8].

We should note that a tropical limit of a matrix soliton solution can only be expected if we arrange the parameters such that exponentials absent in τ are also absent in the numerator of u . Otherwise the solution will exhibit exponential growth (in some space-time direction), in which case the solution should no longer be called a soliton solution.

In the scalar and vector case, inelastic collisions are subject to severe restrictions. As expected, there is more freedom in the full matrix case.

We concentrated on *regular* solutions, for which all summands of τ are positive, so that the tropical limit, defined via Maslov dequantization, of τ makes sense. We did not have to compute this limit directly, however, since instead it is easier to determine the dominating phase regions and then the respective boundaries, which constitute the tropical limit graph. The latter point of view allows a generalization of the tropical limit, which also applies to *singular* solutions, as explained at the end of Section 3.3.1. This allows us to determine, in a simple way, the locus of singularities of a solution.

Nonlinear atomic or molecular chains, modeled by the scalar Boussinesq equation in a continuum limit, disregard a possible polarization of the particles. Taking polarizations or spins into account, such a chain might be described in the continuum limit by a vector or matrix version of the Boussinesq equation.

Similar explorations, as done for matrix Boussinesq equations in this work, should be possible for other integrable equations too, in particular for discrete versions of the Boussinesq equation (see [19, 20, 21], for example).

Acknowledgment. X.-M.C. has been supported by the DAAD Research Grants - Short-Term Grants 2018 (57378443).

Appendix A: Derivation of the binary Darboux transformation for the matrix Boussinesq equation

We recall a binary Darboux transformation result of bidifferential calculus [14, 15].

Theorem A.1. *Let (Ω, d, \bar{d}) be a bidifferential calculus and $\Delta, \Gamma, \lambda, \kappa$ solutions of*

$$\begin{aligned} \bar{d}\Gamma &= \Gamma d\Gamma + [\kappa, \Gamma], & \bar{d}\kappa &= \Gamma d\kappa + \kappa^2, \\ \bar{d}\Delta &= (d\Delta)\Delta - [\lambda, \Delta], & \bar{d}\lambda &= (d\lambda)\Delta - \lambda^2, \end{aligned}$$

and ϕ_0 a solution of

$$d\bar{d}\phi + d\phi K d\phi = 0, \tag{A.1}$$

where $dK = 0 = \bar{d}K$. Let θ and χ be solutions of the linear system

$$\bar{d}\theta = (d\phi_0)K\theta + (d\theta)\Delta + \theta\lambda, \tag{A.2}$$

respectively the adjoint linear system

$$\bar{d}\chi = -\chi K d\phi_0 + \Gamma d\chi + \kappa\chi. \tag{A.3}$$

Let Ω solve the compatible linear system

$$\Gamma\Omega - \Omega\Delta = -\eta K\theta,$$

$$\bar{d}\Omega = (d\Omega)\Delta - (d\Gamma)\Omega + (d\eta)K\theta + \kappa\Omega + \Omega\lambda. \quad (\text{A.4})$$

Where Ω is invertible,

$$\phi = \phi_0 - \theta\Omega^{-1}\chi \quad (\text{A.5})$$

is a new solution of (A.1). □

In the above theorem, we have to assume that all objects are such that the corresponding products are defined and that d and \bar{d} can be applied. Next we define a bidifferential calculus via

$$\begin{aligned} df &= [\partial_x, f]\zeta_1 + \frac{1}{2}[\partial_t + \partial_x^2, f]\zeta_2, \\ \bar{d}f &= \frac{1}{2}[\partial_t - \partial_x^2, f]\zeta_1 + [\beta\partial_x - \frac{1}{3}\partial_x^3, f]\zeta_2, \end{aligned}$$

on the algebra $\mathcal{A} = \mathcal{A}_0[\partial_t, \partial_x]$, where \mathcal{A}_0 is the algebra of smooth functions of two variables, x and t , and ∂_x is the operator of partial differentiation with respect to x . ζ_1, ζ_2 are a basis of a two-dimensional vector space V , from which we form the Grassmann algebra $\Lambda(V)$. d and \bar{d} extend to $\Omega = \mathcal{A} \otimes \Lambda(V)$ in a canonical way, and to matrices with entries in Ω . The equation (A.1) is then equivalent to the matrix potential Bsq $_K$ equation (1.1). Choosing a solution ϕ_0 and setting

$$\Delta = \Gamma = -\partial_x, \quad \lambda = -\frac{1}{3}C\zeta_2, \quad \kappa = -\frac{1}{3}C'\zeta_2,$$

the linear system (A.2) and the adjoint linear system (A.3) lead to (2.1) and (2.2), respectively. Furthermore, (A.4) implies (2.3). According to the theorem, (A.5) yields a new solution of the matrix potential Bsq $_K$ equation (1.1).

References

- [1] Boussinesq J 1872 Théorie des ondes et des remous qui se propagent le long d'un canal rectangulaire horizontal, et communiquant au liquide contenu dans ce canal des vitesses sensiblement pareilles de la surface au fond *J. Math. Pures Appl. 2^e série* **17** 55–108
- [2] Pnevmatikos S 1985 *Singularities & Symmetrical Systems (North-Holland Mathematics Studies vol 103)* ed Pnevmatikos S (Elsevier Science Publishers B.V. (North Holland)) pp 397–437
- [3] Dickey L 2003 *Soliton Equations and Hamiltonian Systems* (Singapore: World Scientific)
- [4] Bogdanov L and Zakharov V 2002 The Boussinesq equation revisited *Physica D* **165** 137–162
- [5] Rasin A and Schiff J 2017 Bäcklund transformations for the Boussinesq equation and merging solitons *J. Phys. A: Math. Theor.* **50** 325202
- [6] Fal'kovich G, Spector M and Turitsyn S 1983 Destruction of stationary solutions and collapse in the nonlinear string equation *Phys. Lett. A* **99** 271–274
- [7] Lambert F and Musette M 1989 On soliton instabilities for the nonlinear string equation *Journal de Physique Colloques* **50 (C3)** C3–33–C3–38
- [8] Dimakis A and Müller-Hoissen F 2018 Matrix KP: tropical limit and Yang-Baxter maps, *Lett. Math. Phys.* <https://doi.org/10.1007/s11005-018-1127-3>

- [9] Dimakis A and Müller-Hoissen F 2017 Matrix Kadomtsev-Petviashvili equation: tropical limit, Yang-Baxter and pentagon maps, *Theor. Math. Phys.* **196** 1164–1173
- [10] Veselov A 2003 Yang-Baxter maps and integrable dynamics *Phys. Lett. A* **314** 214–221
- [11] Goncharenko V and Veselov A 2004 *New Trends in Integrability and Partial Solvability (NATO Science Series II: Math. Phys. Chem.* vol 132) ed Shabat A *et al.* (Dordrecht: Kluwer) pp 191–197
- [12] Tsuchida T 2004 N -soliton collision in the Manakov model *Progr. Theor. Phys.* **111** 151–182
- [13] Ablowitz M, Prinari B and Trubatch A 2004 Soliton interactions in the vector NLS equation *Inv. Problems* **20** 1217–1237
- [14] Dimakis A and Müller-Hoissen F 2013 Binary Darboux transformations in bidifferential calculus and integrable reductions of vacuum Einstein equations *SIGMA* **9** 009
- [15] Chvartatskyi O, Dimakis A and Müller-Hoissen F 2016 Self-consistent sources for integrable equations via deformations of binary Darboux transformations *Lett. Math. Phys.* **106** 1139–1179
- [16] Dimakis A and Müller-Hoissen F 2011 KP line solitons and Tamari lattices *J. Phys. A: Math. Theor.* **44** 025203
- [17] Hirota R and Ito M 1983 Resonance of solitons in one dimension *J. Phys. Soc. Japan* **52** 744–748
- [18] Kodama Y 2010 KP solitons in shallow water *J. Phys. A: Math. Theor.* **43** 434004
- [19] Nijhoff F, Papageorgiou V, Capel H and Quispel G 1992 The lattice Gel'fand-Dikii hierarchy *Inv. Problems* **8** 597–621
- [20] Tongas A and Nijhoff F 2005 The Boussinesq integrable system: compatible lattice and continuum structures *Glasgow Math. J.* **47A** 205–219
- [21] Maruno K I and Kajiwara K 2010 The discrete potential Boussinesq equation and its multi-soliton solutions *Appl. Anal.* **89** 593–609